

# 1 **Losses of soil organic carbon with deforestation in mangroves of Madagascar**

2 *Shortened version for page headings: Losses of soil carbon with mangrove deforestation*

3 Ariane Arias-Ortiz<sup>1,2\*</sup>, Pere Masque<sup>1,3,4,5</sup>, Leah Glass<sup>6</sup>, Lisa Benson<sup>6,7</sup>, Hilary Kennedy<sup>8</sup>, Carlos M.  
4 Duarte<sup>9</sup>, Jordi Garcia-Orellana<sup>1,4</sup>, Claudia R. Benitez-Nelson<sup>10</sup>, Marc S. Humphries<sup>11</sup>, Ismaël  
5 Ratefinjanahary<sup>6</sup>, Jaona Ravelonjatovo<sup>6</sup>, Catherine E. Lovelock<sup>12</sup>

6 <sup>1</sup>Institut de Ciència i Tecnologia Ambientals, Universitat Autònoma de Barcelona, Bellaterra, 08193 Barcelona, Spain.

7 <sup>2</sup>Ecosystem Science Division, Department of Environmental Science, Policy and Management, University of California,  
8 Berkeley, CA, USA.

9 <sup>3</sup>School of Science & Centre for Marine Ecosystems Research, Edith Cowan University, Joondalup WA 6027, Australia.

10 <sup>4</sup>Departament de Física, Universitat Autònoma de Barcelona, Bellaterra, 08193 Barcelona, Spain.

11 <sup>5</sup>International Atomic Energy, 4a Quai Antoine 1er, 98000, Principality of Monaco, Monaco.

12 <sup>6</sup>Blue Ventures Conservation, Villa Bella Fiharena, Rue Gambetta, Lot 269, Toliara 601, Madagascar.

13 <sup>7</sup>Centre for Environment, Fisheries and Aquaculture Science, Lowestoft Laboratory, Lowestoft NR33 OHT, UK.

14 <sup>8</sup>Ocean Sciences, Bangor University, Menai Bridge, Anglesey LL59 5AB, UK.

15 <sup>9</sup>King Abdullah University of Science and Technology (KAUST), Red Sea Research Center (RSRC) & Computational  
16 Bioscience Research Center (CBRC), Thuwal, 23955-6900, Saudi Arabia.

17 <sup>10</sup>School of Earth, Ocean & Environment, University of South Carolina, Columbia, South Carolina 29208, USA.

18 <sup>11</sup>Molecular Sciences Institute, School of Chemistry, University of the Witwatersrand, Johannesburg, South Africa.

19 <sup>12</sup>School of Biological Sciences, The University of Queensland, St Lucia, QLD 4072, Australia.

20

21 \*correspondence to [aariasortiz@berkeley.edu](mailto:aariasortiz@berkeley.edu);

## 22 **Manuscript highlights:**

- 23 • Deforestation led to the loss of 20% of 1-m C stocks and increased soil homogeneity
- 24 • Annual C loss in deforested soils was 4.5 times the C sequestration of intact soils
- 25 • Conservation is temporally more effective than restoration for reducing C emissions

26

27

28

29 **Abstract:** Global mangrove deforestation has resulted in substantial CO<sub>2</sub> emissions to the  
30 atmosphere, but the extent of emissions from soil organic carbon (C) loss remains difficult to assess.  
31 Here, we sampled 5 intact and 5 deforested mangrove plots from Tsimipaika Bay, Madagascar, to  
32 examine the loss of soil C in the 10 years since deforestation. We estimated tree biomass and  
33 analysed grain size, <sup>210</sup>Pb activities, organic C and total nitrogen (N) and their stable isotopes in soils  
34 as well as dissolved organic C in surface waters. Deforested soils revealed evidence of disturbance in  
35 the upper 14 g cm<sup>-2</sup> (~ 40 cm) when compared to reference intact soils, indicated by lower porosity,  
36 higher dry bulk density, an order of magnitude higher soil mixing and loss of C and N despite no  
37 significant soil erosion. While C loss from biomass was unequivocal and was estimated at 130 Mg C  
38 ha<sup>-1</sup>, the C loss from soils was more difficult to assess given the large heterogeneity of intact forest  
39 soils. We estimated that the loss of C due to mangrove clearing and soil exposure over 10 years was  
40 equivalent to ~ 20% of the upper meter soil C stock, and ~ 45% of the C stock accumulated during  
41 the last century. Soil C loss rate was 4.5 times higher than the C sequestration rate in reference intact  
42 soils. These results emphasize the importance of mangrove conservation for CO<sub>2</sub> emissions  
43 mitigation, as they suggest that deforestation-C losses will take substantially longer to offset with  
44 mangrove restoration.

45

46 **Keywords:** Mangroves, deforestation, soil carbon, soil disturbance, CO<sub>2</sub> emissions, Madagascar.

47

48

## 49 **1. Introduction**

50 Mangroves are an important natural resource in the tropics and sub-tropics and provide a  
51 wide range of ecosystem services, including coastal protection, support of fisheries and biodiversity,  
52 nutrient cycling and carbon sequestration (Barbier and others 2011). Their high rates of primary  
53 production and the low rates of organic matter decomposition in their flooded soils lead to  
54 mangroves having some of the highest soil organic carbon (C) stocks among forested ecosystems  
55 (Donato and others 2011; McLeod and others 2011). However, the C stored in their soils is  
56 vulnerable, as mangroves have been widely degraded and converted to alternative land-uses,  
57 resulting in losses of ecosystem services (Alongi 2002) and significant carbon dioxide emissions  
58 (CO<sub>2</sub>) to the atmosphere as previously stored C is remineralized to CO<sub>2</sub> (Lovelock and others  
59 2017b).

60 Consequences of mangrove soil disturbance include subsidence; as roots die, soil volume  
61 collapses and erosion occurs, resulting in loss of soil C. These effects are generally most severe and  
62 longer lasting when caused by anthropogenic versus natural perturbations (Ellison and Farnsworth  
63 1996; Twilley and Day 2012). Soil C loss has been observed, for instance, where soils have been  
64 excavated for the construction of aquaculture ponds (Ong 1993; Kauffman and others 2014). At sites  
65 where mangroves have been removed or uprooted due to human activities or where there have been  
66 intense storms, losses of soil C have been inferred from changes in soil elevation (Cahoon and others  
67 2003; Lang'at and others 2014) or measured as CO<sub>2</sub> efflux (Lovelock and others 2011; Sidik and  
68 Lovelock 2013; Lang'at and others 2014). Although deforestation has been the major cause of forest  
69 loss in the past, there are few studies that have directly measured the change in soil C content in  
70 mangrove soils when forests are degraded, but soils remain in place (Kauffman and others 2016;  
71 Grellier and others 2017; Adame and others 2018).

72           A change in soil C content with mangrove deforestation may occur directly as a consequence  
73 of biomass loss and/or indirectly due to factors affecting soil biogeochemical processes, such as a  
74 change in temperature, physical protection or aeration. For example, variations in mangrove biomass  
75 may reduce inputs of labile C and nutrients from detritus, and increased soil temperature from direct  
76 sun exposure may result in further loss of soil C (Granek and Ruttenberg 2008). Destructive  
77 practices, such as clear cutting, mechanically redistribute C in the soil (Yanai and others 2003;  
78 Zummo and Friedland 2011; Lundquist and others 2014), enhancing oxygen diffusion, altering  
79 microbial communities and organic C remineralization (Kristensen and Alongi 2006). Physical  
80 mixing processes modify the soil structure, transport conditions and soil chemistry, hence potentially  
81 changing the availability of C and N for associated microbial and plant communities (Balesdent and  
82 others 2000). For instance, the addition of biodegradable C to deep stable C stores promotes  
83 microbial respiration of the added and existing organic pools through a priming mechanism (Bianchi  
84 2011), and may accelerate C mineralization beyond that directly derived from mechanical mixing,  
85 contributing to elevated CO<sub>2</sub> emissions from soils. Soil C may also be lost as a consequence of soil  
86 erosion or exported as dissolved C, a process which may be accelerated through direct exposure of  
87 mangrove soils to tidal inundation, rainfall, and waves (Thampanya and others 2006; Labrière and  
88 others 2015), as well as through changes in the composition and biomass of benthic mats driven by a  
89 reduction in mangrove litter loading (Delgado and others 1991; Duke and Wolanski 2001; McKee  
90 2011; Grellier and others 2017).

91

92           Overall, soil C storage represents a balance of C inputs and losses, and because soil is the  
93 largest reservoir of C in many mangrove ecosystems (Donato and others 2011), small changes in its  
94 pool size may translate into significant CO<sub>2</sub> emissions and changes of C fluxes to coastal waters  
95 (Atwood and others 2017; Gillis and others 2017). While it is well established that the harvesting of  
96 terrestrial forests results in a loss of C in organic and mineral soil horizons (Yanai and others 2003;

97 Diochon and others 2009; Zummo and Friedland 2011), the impact of mangrove deforestation on soil  
98 C storage remains limited. Direct assessment of these C losses is important for quantifying CO<sub>2</sub>  
99 emissions from mangrove deforestation and in the value associated with avoiding emissions achieved  
100 through conservation projects (Herr and others 2017). Currently, guidance by the International Panel  
101 for Climate Change on CO<sub>2</sub> emission from coastal wetlands (IPCC 2014) has a “*tier 1*” (i.e., default)  
102 assumption that soil CO<sub>2</sub> emissions and removals are zero for forest management practices in  
103 mangroves. However, the IPCC allows for country-specific “*tier 2*” (i.e., based on direct  
104 assessments) to be adopted by using a C stock-difference method in order to account for any  
105 emissions associated with forest management practices.

106 In this study we aim to quantify the C loss from deforested mangrove soils in northwest  
107 Madagascar. Madagascar contains Africa’s fourth largest national extent of mangroves, representing  
108 approximately 2% of the global mangrove area. Since 1990, more than 20% of Madagascar’s  
109 mangrove ecosystems have been heavily deforested because of the increasing demand for charcoal  
110 and timber by urban populations (Jones and others 2016a), which is the primary cause of mangrove  
111 deforestation in the broader East African region (FAO [Food and Agriculture Organization of the  
112 United Nations] 2007). We sampled soil cores from plots that were either within deforested and  
113 intact forest areas to assess the change of soil C after clearing. We described the physical  
114 characteristics of soils with depth, quantified the variation in C and N contents, and estimated  
115 sediment accumulation rates, soil mixing and potential erosion using the natural radionuclide lead-  
116 210 (<sup>210</sup>Pb) (T<sub>1/2</sub>: 22.3 yr) (Appleby 2001; Arias-Ortiz and others 2018). We also measured  
117 dissolved organic C (DOC) in adjacent coastal surface waters to assess the effects of deforestation on  
118 DOC export 10 y later. Finally, we use our data to estimate the fate and total change of soil C since  
119 mangrove clearance.

120

## 121 **2. Methods**

## 122 2.1 Study site

123 This study was conducted in Tsimipaika Bay (previously referred to as Ambanja Bay; Jones  
124 and others 2016a) in northwest Madagascar (48°28'E, 13°30'S), where anthropogenic mangrove loss  
125 is particularly prominent due to extensive extraction for charcoal and timber (Jones and others 2014).  
126 Together with Ambaro Bay, the Tsimipaika-Ambaro Bay complex forms Madagascar's second most  
127 extensive mangrove ecosystem, with over 40,000 ha of mangrove forests (Jones and others 2014,  
128 2016a). The site is characterized by a humid sub-tropical climate and is influenced by semi-diurnal  
129 tidal ranges varying between maximums of 3.0 – 3.5 m (Rasolofo and Ramilijaona 2009). Mangrove  
130 soils in this region are underlain by alluvial and lake deposits (Jones and others 2016b) flooded by  
131 sea level rise. Contemporary localized mapping supported by field observations indicated that, in  
132 2010, anthropogenic activities had driven substantial deforestation (1,000 ha) mostly near the  
133 southwest region of the peninsula that separates the two bays (Jones and others 2014) (Fig. 1).  
134 Deforestation heavily targets closed canopy mangrove forests followed by open canopy mangroves  
135 (Benson and others 2017), which represent 30 and 56% of the total mangrove area at the Tsimipaika-  
136 Ambaro Bay complex, respectively (Jones and others 2014). *Rhizophora mucronata* is favored for  
137 the charcoal production process, in which trees are felled by hand and carried to nearby temporary  
138 kilns to be carbonized. Non-*Rhizophora* species and unwanted prop roots are burned to heat kilns,  
139 although large volumes of downed wood are often discarded at the site.

140  
141 In November 2016, we sampled soil cores from 5 plots that were cleared between 2006 and  
142 2008 and from 5 plots from an intact forest (Fig. 1). The deforested and forested plots were spatially  
143 separated by ~5 km but had relatively similar environmental conditions such as species composition,  
144 hydroperiod, type and proximity of bedrock and nutrient inputs. Within the sampled plots, four  
145 species of mangroves were present: *Rhizophora mucronata*, *Bruguiera gymnorhiza*, *Ceriops tagal*  
146 and *Sonneratia alba* (Table 1). Intact plots were all well-formed, closed (> 60%) canopy mangroves,

147 consisting of high stature trees (mean height:  $9.0 \pm 0.5$  m) of variable density (800 - 4,700 ha<sup>-1</sup>). The  
148 average diameter at breast height (1.3 m, dbh) was  $12 \pm 2$  cm. Deforested plots used to contain  
149 closed canopy mangrove forests (Blue Ventures, personal communication) and this was evident from  
150 plots comprised of *Ceriops tagal* or *Bruguiera gymnorhiza* where the boles left in place after tree  
151 removal lead to stump densities ranging from 1,000 to 11,400 ha<sup>-1</sup> (Table 1).

152

153 Aboveground tree biomass at each plot (Table S1) was derived from tree diameter and height  
154 measurements using generalized species-specific allometric equations (Clough and Scott 1989; Cole  
155 and others 1999; Chave and others 2005; Kauffman and Donato 2012) and wood density values  
156 (Chave and others 2009; Zanne and others 2009). These equations were chosen based on the region  
157 in which they were developed and the parameters used to derive them, and have been previously  
158 described in Jones and others (2016b) for use in the same area. The maximum tree diameter and  
159 height measured (18 cm and 10 m, respectively) were within the range of trees used to develop the  
160 equations. Tree belowground-biomass was calculated using the generalized equation presented in  
161 Komiyama and others (2005) and equations from Kauffman and Donato (2012) were used to  
162 estimate the biomass of standing dead wood. From biomass density estimates, the total biomass C  
163 stocks (Mg C ha<sup>-1</sup>) were estimated using conversion factors of 0.50 and 0.39 for above and  
164 belowground estimates, respectively (Kauffman and Donato 2012), and should therefore be  
165 considered as approximate estimates of biomass C. Plot size for tree measurements was 100 m<sup>2</sup> and  
166 estimates of biomass and C stocks were scaled to the hectare-level.

167

## 168 **2.2 Sampling and analytical methods**

169 In order to characterize soil biogeochemical properties, PVC tubes (1.5 m long, 6.2 cm inner  
170 diameter) were hammered into mangrove soils (one at each plot; Fig 1), extracted by hand and  
171 transported to the laboratory. Prior to extracting the core, the depth to the sediment surface inside and

172 outside the core was measured in order to assess core shortening during sampling (Glew and others  
173 2001), which averaged  $36 \pm 10\%$  and  $50 \pm 13\%$  in intact and deforested mangrove soils,  
174 respectively. The PVC corers were cut lengthwise, and the soils inside the corers were sliced at 0.5  
175 cm-thick intervals throughout the first 20 cm, and at 1 cm-thick intervals below this depth. Soil depth  
176 layers were weighed wet and then dried at  $60^{\circ}\text{C}$  until a constant weight was achieved. Soil water  
177 content and dry bulk density (DBD) were then calculated. Soil mass per unit area ( $\text{g cm}^{-2}$ ) was also  
178 estimated at each layer by dividing the dry sample mass by the core tube area sampled. The lack of a  
179 reference elevation marker in sampled intact and deforested soils made comparisons of soil  
180 properties based upon depth or volume limited and less precise (Gifford and Roderick 2003; Wendt  
181 and Hauser 2013). We thus used the cumulative mass approach. The cumulative soil mass of each  
182 core was calculated by summing their respective soil mass layers to the bottom of the core. Soil  
183 profiles were displayed in terms of cumulative mass rather than depth to accommodate the impact of  
184 changes in the DBD, and thus surface elevation change, which may occur through soil collapse after  
185 deforestation (Cahoon and others 2003; Krauss and others 2010; Lang'at and others 2014), the  
186 influence of trampling (Kauffman and others 2004), swelling and shrinking with changes in moisture  
187 content (Haines 1923) and due to variable soil shortening and compaction during coring.

188 Soil C and total nitrogen (subsequently notated as N) contents were measured at 1 cm  
189 resolution throughout the upper 30 cm, and in alternate slices every 5 cm below this depth. Prior to  
190 analysis, soil samples were sieved (1.5 mm) to exclude belowground biomass before being ground to  
191 a fine powder. Sub-samples ( $\sim 20$  mg) were weighed into silver cups, acidified with 1 M HCl, dried  
192 at  $60^{\circ}\text{C}$  and then analysed using an elemental analyser (Carlo Erba NA1500). No visual evidence of  
193 effervescence was observed during sample acidification, which indicates that minimal inorganic C  
194 was present. Analytical precision (s.d. of  $n = 26$ ) was  $\pm 0.3\%$  for C,  $\pm 0.02\%$  for N and  $\pm 4$  for molar  
195 C:N ratios. Stable isotopes of sediment C and N ( $\delta^{13}\text{C}$  and  $\delta^{15}\text{N}$ ) were analyzed at one core per  
196 treatment location using an elemental analyzer–isotope ratio mass spectrometer (Hilo Analytical



197 Laboratory) at the University of Hawaii. Sub-samples for stable isotope analyses were encapsulated  
198 in silver cups and acidified as described above. The use of a weak 1 M HCl solution was chosen  
199 following the recommendations in Kennedy and others (2005). Replicate and control samples (NIST  
200 8704) were also run and the accuracy and precision of  $\delta^{13}\text{C}$  and  $\delta^{15}\text{N}$  data were of  $\pm 0.2\%$  and  $\pm$   
201  $0.07\%$ , respectively.

202 Grain size analyses were conducted down core to evaluate potential erosion, which results in  
203 selective and preferential loss of smaller size grain fractions (Arata and others 2016). Sediment  
204 grain-size was measured with a Mastersizer 2000 laser diffraction particle analyzer following  
205 digestion of bulk samples with hydrogen peroxide to remove organic matter. Sediments were  
206 classified as sand (63 - 1,000  $\mu\text{m}$ ), silt (4 - 63  $\mu\text{m}$ ) and clay ( $< 4 \mu\text{m}$ ) (size scale: Wentworth 1922).

207 Specific activities of  $^{210}\text{Pb}$  were measured down core in order to assess soil accumulation  
208 rates and soil erosion. Total  $^{210}\text{Pb}$  was determined through the analysis of its granddaughter  $^{210}\text{Po}$  by  
209 alpha spectrometry after complete sample digestion in a  $\text{HNO}_3\text{:HF}$  mixture (9:3 ml) using an  
210 analytical microwave in the presence of a known amount of  $^{209}\text{Po}$  added as a tracer (Sanchez-Cabeza  
211 and others 1998). Certified reference materials IAEA-447 and IAEA-385 were analyzed alongside  
212 soil samples. Accuracy of the  $^{210}\text{Pb}$ ( $^{210}\text{Po}$ ) measurements averaged  $96 \pm 4\%$ . The specific activities  
213 of  $^{210}\text{Pb}_{\text{xs}}$  used to obtain the age models were determined as the difference between total  $^{210}\text{Pb}$  and  
214  $^{226}\text{Ra}$  (supported  $^{210}\text{Pb}$ ). Specific activities of  $^{226}\text{Ra}$  were determined for selected samples within each  
215 core by gamma-spectrometry through the measurement of  $^{226}\text{Ra}$  decay product emission lines of  
216  $^{214}\text{Pb}$  at 295 and 352 keV and using calibrated geometries in a HPGe detector (CANBERRA, Mod.  
217 SAGe Well). Total  $^{210}\text{Pb}$  activities at depth derived by alpha and  $^{226}\text{Ra}$  specific activities via gamma  
218 were within error of one another confirming agreement between alpha and gamma methods. Mean  
219 sediment accumulation rates over the last several decades to century were estimated for intact  
220 mangrove soils using the Constant Flux:Constant Sedimentation (CF:CS) model applied below the  
221 surface mixed layer (Krishnaswamy and others 1971) following the recommendations in Arias-Ortiz

222 and others (2018). Mass accumulation rates (MAR) are expressed in cumulative dry mass units (g  
223  $\text{cm}^{-2} \text{y}^{-1}$ ) and accretion rates (SAR) in  $\text{mm y}^{-1}$ . Carbon accumulation rates (CAR) were estimated as  
224 the product of the fraction of %C accumulated down to the excess  $^{210}\text{Pb}$  horizon ( $C_t$ ) by the MAR of  
225 that period ( $MAR_t$ ):

$$226 \quad \quad \quad CAR = C_t \cdot MAR_t \quad \quad \quad (\text{Eq.1})$$

227 The same equation can be applied to estimate N accumulation rates. Potential soil erosion triggered  
228 by mangrove removal was assessed by comparing the  $^{210}\text{Pb}_{\text{xs}}$  inventories ( $^{210}\text{Pb}_{\text{xs}}$  activity per unit  
229 area) at deforested mangrove soils against the inventories measured in intact mangrove soils.

230 Soil C stocks were quantified using equivalent soil mass layers rather than depth to account  
231 for variations in bulk density across sites and down core. The soil mass layers used as the basis for  
232 comparison were  $14 \text{ g cm}^{-2}$  (upper), which represented soils accumulated in the last century (based  
233 on the average  $^{210}\text{Pb}_{\text{xs}}$  horizon),  $14 - 45 \text{ g cm}^{-2}$  (bottom), and  $45 \text{ g cm}^{-2}$  (total), which was the average  
234 cumulative mass equivalent to approximately 1 m of soil. Estimates of soil C stocks integrated to a  
235 depth of 1 m are also reported for comparison to global estimates. For the latter purpose, we  
236 corrected soil depth for core shortening by linearly distributing the spatial discordance between the  
237 length of the recovered soil and the depth penetrated by the core tube to the sliced soil layers  
238 following Morton and White (1997). We acknowledge that by using a whole-core value, differential  
239 interval shortening with depth might be underestimated and could lead to erroneous conclusions  
240 regarding the magnitude of deformation and the need for depth corrections. Here, cumulative mass  
241 intervals were used as a reference for detailed depth-dependent quantitative comparisons. A different  
242 coring method that reduces shortening (Hargis and Twilley 1994) or the taking of several intermittent  
243 measurements of soil shortening during coring (Morton and White 1997) would have been necessary  
244 to use depth-based approaches.

245 Surface water samples were collected over a tidal cycle at 8 sites along the shore adjacent to  
246 the intact (stations 1-4) and deforested (stations 5-8) mangrove areas. The intact sites were sampled

247 during the flood to high slack tide. The deforested sites were sampled during the ebb to low slack  
248 tide. Samples for total organic C were collected in 20 mL combusted glass vials, acidified to pH of 2  
249 and stored at 4°C until analysis. Samples were analyzed as both filtered (using acid-washed and pre-  
250 combusted syringe GF/F filters) and unfiltered samples. Total and dissolved organic C were  
251 measured using high temperature (720°C) catalytic oxidation (Pt-alumina) on a Shimadzu TOC-V  
252 CPN analyzer (Benner and Strom 1993). Analytical replication (5 injections, 100  $\mu$ L) of consensus  
253 reference material (Florida Straight at 700 m, DOC-CRM program) was run every 10 samples. High  
254 concentrations were also measured diluted with distilled and deionized water. Total organic C versus  
255 filtered DOC concentrations, and high concentration versus diluted samples were found to be the  
256 same within error ( $\pm 50 \mu\text{mol C L}^{-1}$ ).

257

### 258 **2.3 Statistics**

259 Water content, DBD, C and N content and molar C:N ratios in soils as well as DOC  
260 concentrations in surface waters were not normally distributed, and thus non-parametric tests were  
261 used to assess significant differences between intact and deforested areas (Mann-Whitney test) at a  
262 level of significance of  $< 0.05$ . We used principal component analysis (PCA) to assess the  
263 relationship between soil properties and the two areas studied (intact and deforested mangroves).  
264 Sediment grain size,  $^{210}\text{Pb}_{\text{xs}}$  inventories,  $\delta^{13}\text{C}$  and  $\delta^{15}\text{N}$ , and stocks did follow a normal distribution,  
265 hence a two-sample t-test was used to assess significant differences between intact and deforested  
266 mangrove soils. Mean  $\pm$  SE values are reported throughout the manuscript together with median  
267 values where variables were not normally distributed.

268

### 269 **2.4 Emissions from mangrove forest deforestation**

270 We analysed C losses and potential emissions from mangrove deforestation based upon the  
271 variation in C content in the mangrove soil profiles between intact and deforested soils. Likewise,

272 biomass C loss was estimated as the difference between vegetation C stocks in intact and deforested  
273 plots. The losses of C were reported as CO<sub>2</sub> equivalents (CO<sub>2</sub>e), obtained by multiplying C loss  
274 values by 3.67, i.e., the molecular ratio of CO<sub>2</sub> to C. The mean annual rate of C loss from deforested  
275 soils was estimated as the total soil C stock loss divided by the time elapsed since disturbance (10  
276 years).

277

### 278 **3. Results**

279 The effect of deforestation was obvious due to differences in mangrove vegetation compared  
280 to undisturbed sites. Total estimated biomass C stocks in intact plots ranged from 113 to 254 Mg C  
281 ha<sup>-1</sup>, while in deforested plots these were substantially lower (0.06 to 9.5 Mg C ha<sup>-1</sup>) and contained  
282 negligible belowground biomass (i.e., roots) (Table 1 and Table S1). The effects of deforestation  
283 were less clear in soils from deforested mangroves, which contained similar average C and N  
284 contents to intact mangroves over the total soil profile ( $P > 0.05$ ) (Table 2). This was in part because  
285 variability in soil properties within the five intact mangrove cores was large and data followed a  
286 bimodal distribution (Fig. S1). Intact soils Cc19 and Cc20, hereafter referred to as high-DBD intact  
287 soils, were depleted in water content and had significantly higher soil DBD and lower C and N  
288 contents relative to deforested soils ( $P < 0.01$ ). In contrast, intact plots Cc18, Cc28 and Cc29,  
289 hereafter referred to as low-DBD intact soils, had significantly lower DBD and higher water, C and  
290 N contents than deforested soils ( $P < 0.01$ ). As a consequence, physico-chemical properties of  
291 deforested soils fell between those of high-DBD and low-DBD intact soils (Table 2).

292 Multivariate analyses further confirmed that soils from intact mangroves were represented by  
293 two clusters of data and that deforested soils were comparable to a mixture of low- and high-DBD  
294 intact soils, with characteristics closer to low-DBD intact soils (Fig. 2). Principal components Pc1  
295 and Pc2 explained 75% of the total variance among sampled soils. Pc1 comprised 50% of the  
296 variance and was strongly correlated with soil DBD ( $r = -0.90$ ), water, and C and N contents ( $r =$

297 0.95,  $r = 0.95$  and  $r = 0.94$ , respectively). Pc2 explained 25% of the variance and was strongly  
298 correlated with clay ( $r = 0.91$ ) and moderately correlated with C:N ratios ( $r = 0.53$ ).

299

300 Concentrations of DOC in surface ocean waters varied widely between stations, with 8 times  
301 higher median concentrations measured during ebb tide (Fig. 3). Stations 1- 3, adjacent to the intact  
302 mangrove area and sampled during the flood tide, had the lowest DOC concentrations ( $320 \pm 30$   
303  $\mu\text{mol C L}^{-1}$ ) contrasting with those measured at station 4 ( $3,500 \pm 50 \mu\text{mol C L}^{-1}$ ), also adjacent to  
304 the intact forest, but sampled during the high slack to ebb tide. All surface waters nearshore of the  
305 deforested mangroves were sampled during the ebb to low slack tide, leading to some of the highest  
306 DOC concentrations, ranging between 1,000 and 19,400  $\mu\text{mol C L}^{-1}$ . Due to tidally-driven  
307 variability, no significant differences could be observed in median surface water DOC concentrations  
308 between intact and deforested nearshore areas ( $P = 0.19$ ).

309

### 310 **3.1 Soil physico-chemical properties downcore**

311 Changes in soil physico-chemical properties over the soil profile were observed in low-DBD  
312 intact and deforested mangrove soils only. In soils from low-DBD intact mangroves, DBD increased  
313 linearly and water content decreased with soil cumulative mass (or depth in  $\text{g cm}^{-2}$ , hereafter).  
314 Deforested soils, however, displayed a constant and significantly higher DBD, with decreasing water  
315 content over the upper  $14 \text{ g cm}^{-2}$  (or  $\sim 40 \text{ cm}$ ) ( $P < 0.01$ ; Table S2) (Fig. 4a and b).

316

317 Carbon and N content (%DW) in low-DBD intact mangrove soils decreased steadily  
318 downcore, opposite to the pattern observed in deforested soils, which increased with depth in the  
319 upper  $14 \text{ g cm}^{-2}$  (Fig. 4c and d). The mean soil C content of low-DBD intact soils was  $8.4 \pm 0.2\% \text{ C}$   
320 in the upper  $14 \text{ g cm}^{-2}$ , 2-fold higher than that in deforested soils ( $4.7 \pm 0.2\% \text{ C}$ ). Below this horizon,  
321 however, no significant differences were observed in water, C or N contents between deforested and

322 low-DBD intact soils (Fig. 4) (Table S2). In contrast, soil properties of high-DBD intact soils  
323 remained relatively constant and differed significantly from those in low-DBD intact and deforested  
324 soils throughout the soil profile (Table 2).

325 Molar C:N ratios were high in all sampled soils with averages ranging from 29 to 33, and  
326 increased downcore in low-DBD intact and deforested soils. Correlation between C:N ratios and soil  
327 cumulative mass was positive and significant in all treatments ( $P < 0.001$ ) except for the high-DBD  
328 intact soils ( $P > 0.05$ ). The relationship was strongest in the upper 14 g cm<sup>2</sup> of deforested soils ( $r_s =$   
329 0.54) and the slope higher than in the low-DBD intact soils ( $r_s = 0.41$ ) (Fig. S2). Although,  
330 deforested soils were characterized by higher average C:N molar ratios over the total soil profile no  
331 significant differences were observed in bottom layers between low-DBD intact and deforested soils  
332 (Table S2).

333 Stable isotopes of C and N were analysed for one low-DBD intact and one deforested soil.  
334 Both mangrove soils showed  $\delta^{13}\text{C}$  values close to -28‰ although C in the deforested soil had lighter  
335 average  $\delta^{13}\text{C}$  values ( $-28.16 \pm 0.05\text{‰}$ ) than C in the intact soil ( $-27.5 \pm 0.1\text{‰}$ ) ( $P < 0.001$ ). In  
336 contrast, the  $\delta^{15}\text{N}$  signal averaged  $0.92 \pm 0.10\text{‰}$  and was not significantly different between the two  
337 soil types ( $P = 0.70$ ). Soil C in low-DBD intact soil showed  $\delta^{13}\text{C}$  values that became slightly heavier  
338 (+1.2‰) over the upper layer and relatively constant in the bottom layer (Fig. 4c). The deforested  
339 soil showed an initial change from heavy to lighter  $\delta^{13}\text{C}$  values at  $\sim 3 \text{ g cm}^{-2}$  before becoming  
340 heavier downcore (Fig. 4d).  $\delta^{15}\text{N}$  showed a similar pattern as  $\delta^{13}\text{C}$  in the intact soil but showed  
341 scattered values down core in the deforested soil.

342

343 The grain size distribution of all intact and deforested mangrove soils was relatively  
344 homogeneous over the soil profile. Silt accounted for  $52 \pm 5\%$  and  $58 \pm 6\%$  of dry weight,  
345 respectively. However, the average clay content ( $< 4 \mu\text{m}$ ) in deforested soils ( $28 \pm 1\%$ ) was about  
346 twice that of high-DBD ( $11 \pm 1\%$ ) and low-DBD intact soils ( $15 \pm 1\%$ ) (Fig. S3). No significant

347 differences in clay content were observed with depth in any of the sampled soils ( $P > 0.01$ ; Table  
348 S2).

349

### 350 **3.2 $^{210}\text{Pb}$**

351 In all intact mangrove soils, the excess  $^{210}\text{Pb}$  ( $^{210}\text{Pb}_{\text{xs}}$ ) specific activity decreased from the  
352 surface to below detection at depths between 7 and 17  $\text{g cm}^{-2}$  (Fig. 5a). The CF:CS model was used  
353 to estimate average mass accumulation rates over this depth horizon (Krishnaswamy and others  
354 1971), which ranged between  $0.070 \pm 0.014 \text{ g cm}^{-2} \text{ y}^{-1}$  and  $0.223 \pm 0.012 \text{ g cm}^{-2} \text{ y}^{-1}$  (or  $0.85 \pm 0.11$   
355 and  $8.4 \pm 0.4 \text{ mm y}^{-1}$ ; Table 3) at intact sites. In deforested mangrove soils,  $^{210}\text{Pb}_{\text{xs}}$  horizons were  
356 reached at 10 to 26  $\text{g cm}^{-2}$  ( $18 \pm 3 \text{ g cm}^{-2}$ ) but intense soil mixing, indicated by uniform specific  
357 activities of  $^{210}\text{Pb}_{\text{xs}}$  throughout deforested soil profiles, precluded the determination of a valid age  
358 model and sediment accumulation rates at these sites. Indeed, the cumulative mass of the soil mixed  
359 layer was on average 10 times greater in deforested than in intact soils ( $14 \text{ g cm}^{-2}$  versus  $1.4 \text{ g cm}^{-2}$ )  
360 (Table 3). The  $^{210}\text{Pb}_{\text{xs}}$  inventories in intact mangrove soils varied widely (600 - 4,800  $\text{Bq m}^{-2}$ ),  
361 although the average ( $2,210 \pm 800 \text{ Bq m}^{-2}$ ) was not significantly different to that observed in  
362 deforested mangrove soils (mean  $1,930 \pm 220 \text{ Bq m}^{-2}$ ) ( $P = 0.74$ ), where the  $^{210}\text{Pb}_{\text{xs}}$  inventory was  
363 redistributed over the soil profile via mixing. It should be noted that high-DBD intact soils contained  
364 the lowest  $^{210}\text{Pb}_{\text{xs}}$  inventories ( $600 \pm 100 \text{ Bq m}^{-2}$ ). This could potentially mask significant differences  
365 between intact and deforested  $^{210}\text{Pb}_{\text{xs}}$  inventories, and therefore, erosion patterns using the targeted  
366 inventory comparison. However, the mean  $^{210}\text{Pb}_{\text{xs}}$  inventory of low-DBD intact soils was also not  
367 significantly different than that of deforested soils ( $P = 0.08$ ), indicating the lack of erosion at  
368 deforested sites relative to reference intact sites.

369

### 370 **3.3 C and N accumulation rates and stocks**

371 Mean soil C and N burial rates during the last century within the closed canopy forest ranged  
372 from 18 to 176 g C m<sup>-2</sup> y<sup>-1</sup> and from 0.7 to 7.2 g N m<sup>-2</sup> y<sup>-1</sup>, respectively, not including belowground  
373 biomass accumulation. In low-DBD intact soils, C and N burial rates averaged 110 ± 40 g C m<sup>-2</sup> y<sup>-1</sup>  
374 and 4 ± 2 g N m<sup>-2</sup> y<sup>-1</sup>, respectively and were similar to burial rates estimated globally (Breithaupt and  
375 others 2012) but 5 times higher than those found in high-DBD intact soils (Table 4). In deforested  
376 plots, soil C and N burial rates could not be estimated due to soil mixing over the entire <sup>210</sup>Pb<sub>xs</sub>  
377 record.

378  
379 Evidence for soil C and N losses was clear between deforested and low-DBD intact soils in  
380 the upper 14 g cm<sup>-2</sup>, which encompasses soils accumulated during the last century, as indicated by the  
381 average depth of <sup>210</sup>Pb<sub>xs</sub> horizon in all sampled soils (Table 3). Over this depth and equivalent period  
382 of accumulation, stocks of C and N in deforested soils were half those of low-DBD intact soils  
383 (Table 4). No significant differences, however, were observed if high-DBD intact soils were included  
384 in the comparison or if stock comparisons were made over the upper 45 g cm<sup>-2</sup> or 1 m of soil (*P* >  
385 0.05 in all cases).

386

#### 387 **4. Discussion**

388 Changes in soil C stocks following deforestation can be an important component of the  
389 ecosystem C budget and therefore climate mitigation. This is particularly true for ecosystems such as  
390 mangrove forests. In Madagascar, clearing and harvesting of the mangrove forest between 1990 and  
391 2010 has resulted in an estimated net loss of ~ 21% of mangrove cover (Jones and others 2016a), but  
392 the effects of these activities on soil C storage are poorly known. Carbon losses from soils following  
393 mangrove clearance are more difficult to assess than aboveground stocks. The slow rate at which soil  
394 C stocks change and their inherently large spatial variability make quantification of recent changes  
395 unclear, especially when soils have remained on site but have been mixed and/or compacted and



396 reference soil depths are no longer valid. As evidenced from the low- and high-DBD intact mangrove  
397 soils in this study and reported elsewhere (Chmura and others 2003; Ferreira and others 2010;  
398 Kauffman and others 2014; Otero and others 2017), intact mangrove soils are heterogeneous. Soil  
399 heterogeneity can be increased by mangroves themselves through biotic processes such as  
400 colonization, root activity and distribution, and decomposition (Boto and Wellington 1984). It can  
401 also occur from environmental processes such as coastal evolution and changes in creek  
402 configuration (Macnae 1969; Semeniuk 1996; Ferreira and others 2010), differences in tidal water  
403 flooding or sediment supply (Chmura and others 2003). We observed a wide range and variability in  
404 soil physico-chemical properties and C and N stocks and accumulation rates in soils from intact  
405 mangroves in Tsimipaika Bay that were independent of aboveground biomass, mangrove species or  
406 distance from shore, but showed a 5-fold difference in soil accretion rates between soils in high- and  
407 low-DBD intact mangrove plots. In contrast, soil properties including  $^{210}\text{Pb}_{\text{xs}}$  inventories and C and  
408 N profiles appeared spatially homogeneous among cleared soils, suggesting that deforestation and  
409 the continuous exposure of soils caused a general loss of natural variability. This pattern was also  
410 reported by Stoke and Harris (2015) in New Zealand and, although often overlooked, may be an  
411 additional sign of ecosystem function and service loss (Stover and Henry 2018).

412         The effects of deforestation and the continuous exposure of soils over 10 years were clear in  
413 the upper  $14 \text{ g cm}^{-2}$  (or apparent  $\sim 40 \text{ cm}$ ). Over this depth, all deforested soils showed evidence of  
414 disturbance as indicated by lower water content, higher DBD, 10-times higher soil mixing and a  
415 higher depletion of C and N contents at the surface. Pre-existing soil properties and C and N stocks  
416 were unknown at deforested plots. However, the strong convergence of soil properties between  
417 deforested and low-DBD intact soils below  $14 \text{ g cm}^{-2}$  (Fig. 4; Table S2) allowed us to use the latter  
418 as a reference for pre-deforestation conditions. This approach has been used previously (Grellier and  
419 others 2017), and gives first-order estimates of biomass and soil C and N loss. Both low-DBD intact  
420 and deforested soils showed isotopic  $\delta^{13}\text{C}$  values of sedimentary organic C similar to those of

421 mangrove vegetation (-29.4 to -27‰; Bouillon and others 2008b) suggesting that the source of  
422 organic matter was predominantly of mangrove origin at both sites. The enrichment of  $\delta^{13}\text{C}$  and  $\delta^{15}\text{N}$   
423 with depth in low-DBD intact soils was consistent with organic matter decomposition with age  
424 (Fourqurean and Schrlau 2003) and with the Suess effect, i.e., the temporal decrease in atmospheric  
425  $\text{CO}_2$   $\delta^{13}\text{C}$  signature from the burning of fossil fuels (Keeling 1979). This was not observed in the  
426 deforested soil because of sediment mixing in the upper layers. The 10-fold larger soil mixing at  
427 deforested sites could have been caused by trampling by harvesters and dragging of logs during  
428 clearcutting. As shown in the felling of terrestrial forests, most soil damage occurs during wood  
429 transportation from the stump area to the landings (Jamshidi and others 2008; Cambi and others  
430 2015). In addition, 10 years of subsequent exposure of reworked soils could have led to increased  
431 erosion of cleared soils with tides and run off as observed in Grellier and others (2017) two years  
432 after mangrove clearing. However, unlike the study of Grellier et al. (2018) in Vietnam, our data do  
433 not show a winnowing of fine particles at deforested sites. Indeed, our deforested soils contained  
434 twice as much clay per soil volume as intact soils throughout the soil profile suggesting that their  
435 location at the bottom of the U-shaped bay might favor the retention of sediments regardless of  
436 mangrove loss. This is confirmed by similar average  $^{210}\text{Pb}_{\text{xs}}$  inventories measured within deforested  
437 and low-DBD intact soils. Despite the large variability at intact sites, results suggest that net soil  
438 erosion was not enhanced at deforested sites, hence could not explain the depletion of C and N  
439 observed in the upper  $14 \text{ g cm}^{-2}$ .

440 In our study, the observed C depletion measured in the upper  $14 \text{ g cm}^{-2}$  of deforested soils  
441 could have occurred largely because of the lack of new litter supply and the enhanced C  
442 remineralization promoted by soil physical mixing and the exposure of deforested surface soils to  
443 direct solar radiation after canopy loss (Bosire and others 2003; Lovelock and others 2017a). Soil  
444 mixing can impact C processing in multiple ways: by aeration, by mixing labile organic matter to  
445 deeper layers as well as by breaking the soil structure and exposing organic material previously

446 protected by burial (Burdige 2007; Middelburg 2018). All these processes promote C mineralization  
447 and CO<sub>2</sub> emissions to the atmosphere (Lovelock and others 2017a). Assuming that low-DBD intact  
448 soils best represent deforested soils before mangrove clearance, we estimated that soil C loss caused  
449 by deforestation accounted for  $50 \pm 14 \text{ Mg C ha}^{-1}$ , as indicated by the comparison of C stocks over  
450 the upper  $14 \text{ g cm}^{-2}$  (Table 4). This C loss would have occurred at a mean rate of  $5.0 \pm 1.4 \text{ Mg C ha}^{-1}$   
451  $\text{yr}^{-1}$  during the 10-yr following clearcutting, which is 4.5 times higher than the annual C  
452 sequestration rate estimated in low-DBD intact soils.

453         Roughly 20% of the upper 1-m C stock, and 45% of that accumulated in the last century,  
454 would have been lost since deforestation relative to low-DBD intact soils. The magnitude of C loss  
455 in the upper  $14 \text{ g cm}^{-2}$  was, however, as important as the variability of the C stocks in the upper  $45 \text{ g}$   
456  $\text{cm}^{-2}$  (apparent  $\sim 1 \text{ m}$ ) of low-DBD and deforested soils. This may explain why differences in soil C  
457 stocks at a depth of 1 meter could not be detected in this study and others (Lang'at and others 2014),  
458 unless specific soil mass-depth increments that encompass similar accumulation periods were  
459 analyzed. Proportional changes in N stocks were comparable. Results indicated a preferential loss of  
460 N with age (or depth) under natural conditions that was enhanced with disturbance as deforested  
461 soils showed a greater increase in average C:N ratios than intact soils throughout the upper  $14 \text{ cm}^{-2}$   
462 (Fig. S2). Soil C loss occurred in addition to the loss from standing biomass, which was estimated at  
463  $130 \pm 14 \text{ Mg C ha}^{-1}$  (Fig. 6). Soil C and N losses (versus tree biomass) could have been lower if  
464 deforestation had occurred for mangroves in high-DBD intact plots given their smaller organic C and  
465 N soil content (Lovelock and others 2017a).

466

467         Pathways for soil C loss likely include atmospheric emissions as CO<sub>2</sub> and lateral export as  
468 dissolved C to coastal waters. Most research has focused on constraining C losses from soils as  
469 fluxes of CO<sub>2</sub> following disturbance (e.g., references in Table 5). For comparison, the mean C loss  
470 rate estimated in deforested soils here is equivalent to emissions of  $18 \pm 5 \text{ Mg CO}_2 \text{ ha}^{-1} \text{ yr}^{-1}$ , which

471 compare well with CO<sub>2</sub> efflux measurements after mangrove clearing reported by others (e.g.,  
472 Lang'at and others 2014; Bulmer and others 2015; Grellier and others 2017) and is similar to CO<sub>2</sub>  
473 emissions inferred from peat collapse due to hurricane damage (Cahoon and others 2003) and from  
474 stock change methods after conversion to cattle pastures (Kauffman and others 2016) (Table 5).  
475 However, our estimated emissions were about 4 times lower than those reported when soils were  
476 excavated and converted to shrimp ponds (Sidik and Lovelock 2013; Kauffman and others 2014,  
477 2018).

478 Lateral fluxes of dissolved C from cleared mangroves have been rarely considered (Sippo and  
479 others 2019), despite this being the major fate of C from healthy mangrove forests (Bouillon and  
480 others 2008; Maher and others 2018). Although our data were limited, DOC concentrations of waters  
481 nearshore of the deforested and intact forests were very high, even during flood tide, far exceeding  
482 those typical of seawater and coastal waters (~100 and 200  $\mu\text{mol C L}^{-1}$ , respectively; Barrón and  
483 Duarte 2015), which confirms the importance of mangrove forests, whether intact or degraded, as a  
484 source of DOC to the coastal ocean. The lack of samples taken along river sources and coastal areas  
485 at the same tidal stage precluded assessing the effect of mangrove deforestation on the magnitude of  
486 DOC export. However, because mangrove deforestation limits the supply of new C inputs to the  
487 forest floor, the presence of high DOC concentrations (median: 2,000  $\mu\text{mol C L}^{-1}$ ) in waters  
488 nearshore of the cleared area even 10 years after deforestation may suggest that existing soil C  
489 reserves are being depleted. This is consistent with the findings by Maher and others (2017), who  
490 showed that even aged sequestered C in mangroves is susceptible to remineralization and export to  
491 the coastal ocean. This process reintroduces aged C into the modern C cycle and thus could lead to  
492 increased CO<sub>2</sub> emissions in coastal waters if bioavailable and oxidized (Drake and others 2019).

493

494 Mangrove deforestation promotes changes in soil physico-chemical properties and functions  
495 (soil C storage, nutrient processing and vertical accretion) (Grellier and others 2017; Otero and

496 others 2017) that enhance the susceptibility of C stocks to remineralization, resulting in potential  
497 changes in C fluxes to the coast and large amounts of CO<sub>2</sub> to the atmosphere. Using “*tier 2*”  
498 approaches, we estimate that mangrove deforestation for timber and charcoal in Tsimipaika Bay has  
499 resulted in measurable reductions in total ecosystem C stocks that represents a combined potential  
500 loss of  $180 \pm 20$  Mg C ha<sup>-1</sup> from standing biomass and soil organic C stocks in the 10 years since  
501 clearing. While C losses from standing biomass are unequivocal and could contribute significantly to  
502 CO<sub>2</sub> emissions if harvested timber is used as fuel-wood, emissions from soils are more difficult to  
503 assess because of the large soil heterogeneity of intact mangrove forests and the partial export of C to  
504 adjacent aquatic coastal systems. However, our data show that even in the absence of excavation of  
505 soils (e.g. for aquaculture ponds, Kauffman and others 2014) or soil erosion, C losses would have  
506 occurred at a rate that is 4.5 times that which C accumulates in soils of intact closed-canopy forests.  
507 In Tsimipaika-Ambaro Bay, closed-canopy mangrove forests cover 14,000 ha in contrast to 1,000 ha  
508 of deforested soils, which thereby reduce the annual C sequestration capacity of the dense mangrove  
509 ecosystem by 32%. Nation-wide, Madagascar has lost 20,300 ha of mangroves between 2000 and  
510 2010 (Jones and others 2016a). If our results are broadly representative, C loss from cleared  
511 mangrove soils could be significant and account for approximately 20% of total national C emissions  
512 from fossil fuel combustion over that 10 year period (Boden and others 2017). Although rates of  
513 mangrove deforestation have slowed in the last decade (Hamilton and Casey 2016), deforestation of  
514 mangroves is still a nationally important source of emissions for many nations, particularly those  
515 with high rates of deforestation and moderate emissions from other sectors (Taillardat and others  
516 2018). Our results show the importance of avoiding CO<sub>2</sub> emissions associated with mangrove  
517 deforestation, particularly, given that establishing high rates of carbon uptake through restoration of  
518 mangroves can take decades (Osland and others 2012). Thus, conservation is an effective mechanism  
519 for reducing CO<sub>2</sub> emissions. Conservation projects seeking to account for C emissions and removals

520 should take into consideration avoided emissions from soils as well as from loss of biomass, even in  
521 cases where excavation of soils has not taken place.

522

### 523 **Data availability**

524 Data supporting the findings of this study (DBD, water content, grains size distribution, C and N  
525 contents,  $\delta^{13}\text{C}$  and  $\delta^{15}\text{N}$ ,  $^{210}\text{Pb}$  and DOC) are available at <https://ddd.uab.cat/record/216456> with the  
526 identifier doi:10.5565/ddd.uab.cat/216456

527

### 528 **Acknowledgements**

529 We thank the Blue Ventures team in Madagascar and Samantha Ridgway and Gloria Salgado from  
530 Edith Cowan University for their help in the field and lab work. Funding was provided to PM and  
531 JGO by the Generalitat de Catalunya (Grant 2017 SGR-1588) and to PM through an Australian  
532 Research Council LIEF Project (LE170100219). Funding was provided to MH and CBN through a  
533 South African NRF Research Development grant (Grant No: 105724). Blue Ventures was funded by  
534 the GEF Blue Forests Project. This work is contributing to the ICTA ‘Unit of Excellence’ (MinECo,  
535 MDM2015-0552). AA-O was supported by “Obra Social la Caixa” (LCF/BQ/ES14/10320004) and  
536 by the NOAA C&GC Postdoctoral Fellowship Program administered by UCAR-CPAESS under  
537 award #NA18NWS4620043B.

538

### 539 **References**

- 540 Adame MF, Zakaria RM, Fry B, Chong VC, Then YHA, Brown CJ, Lee SY. 2018. Loss and recovery of  
541 carbon and nitrogen after mangrove clearing. *Ocean Coast Manag* 161:117–26.
- 542 Alongi DM. 2002. Present state and future of the world’s mangrove forests. *Environ Conserv* 29:331–49.

- 543 Appleby PG. 2001. Chronostratigraphic Techniques in Recent Sediments. In: Tracking Environmental Change  
544 Using Lake Sediments. Vol. 1. Springer Netherlands. pp 171–203.
- 545 Arata L, Meusburger K, Frenkel E, A'Campo-Neuen A, Iurian AR, Ketterer ME, Mabit L, Alewell C. 2016.  
546 Modelling Deposition and Erosion rates with RadioNuclides (MODERN) - Part 1: A new conversion  
547 model to derive soil redistribution rates from inventories of fallout radionuclides. J Environ Radioact  
548 162–163:45–55.
- 549 Arias-Ortiz A, Masqué P, Garcia-Orellana J, Serrano O, Mazarrasa I, Marbà N, Lovelock CE, Lavery P,  
550 Duarte CM. 2018. Reviews and syntheses: <sup>210</sup>Pb-derived sediment and carbon accumulation rates in  
551 vegetated coastal ecosystems: setting the record straight. Biogeosciences 15:6791–818.
- 552 Atwood TB, Connolly RM, Almahasheer H, Carnell PE, Duarte CM, Ewers Lewis CJ, Irigoien X, Kelleway  
553 JJ, Lavery PS, Macreadie PI, Serrano O, Sanders CJ, Santos I, Steven ADL, Lovelock CE. 2017. Global  
554 patterns in mangrove soil carbon stocks and losses. Nat Clim Chang 7:523–8.
- 555 Balesdent J, Chenu C, Balabane M. 2000. Relationship of soil organic matter dynamics to physical protection  
556 and tillage. Soil Tillage Res 53:215–30.
- 557 Barbier EB, Hacker SD, Kennedy C, Koch EW, Stier AC, Silliman BR. 2011. The value of estuarine and  
558 coastal ecosystem services. Ecol Monogr 81:169–93.
- 559 Barrón C, Duarte CM. 2015. Global Biogeochemical Cycles from the coastal ocean. Global Biogeochem  
560 Cycles 29:1725–38.
- 561 Benner R, Strom M. 1993. A critical evaluation of the analytical blank associated with. MarChem 41:153–60.
- 562 Benson L, Glass L, Jones TG, Ravaoarinosihoarana L, Rakotomahazo C. 2017. Mangrove carbon stocks  
563 and ecosystem cover dynamics in southwest Madagascar and the implications for local management.  
564 Forests 8:1–21.
- 565 Bianchi TS. 2011. The role of terrestrially derived organic carbon in the coastal ocean: A changing paradigm  
566 and the priming effect. Proc Natl Acad Sci 108:19473–81.

- 567 Boden TA, Marland G, Andres RJ. 2017. Global, Regional, and National Fossil-Fuel CO<sub>2</sub> Emissions.  
568 [https://cdiac.ess-dive.lbl.gov/trends/emis/overview\\_2014.html](https://cdiac.ess-dive.lbl.gov/trends/emis/overview_2014.html). Last accessed 13/10/2019
- 569 Bosire JO, Dahdouh-Guebas F, Kairo JG, Koedam N. 2003. Colonization of non-planted mangrove species  
570 into restored mangrove stands in Gazi Bay, Kenya. *Aquat Bot* 76:267–79.
- 571 Boto K, Wellington J. 1984. Soil characteristics and nutrient status in a northern Australian mangrove forest.  
572 *Estuaries*.
- 573 Bouillon S, Borges A V., Castañeda-Moya E, Diele K, Dittmar T, Duke NC, Kristensen E, Lee SY, Marchand  
574 C, Middelburg JJ, Rivera-Monroy VH, Smith TJ, Twilley RR. 2008. Mangrove production and carbon  
575 sinks: A revision of global budget estimates. *Global Biogeochem Cycles* 22:1–12.
- 576 Breithaupt JL, Smoak JM, Smith TJ, Sanders CJ, Hoare A. 2012. Organic carbon burial rates in mangrove  
577 sediments: Strengthening the global budget. *Global Biogeochem Cycles* 26.
- 578 Bulmer RH, Lundquist CJ, Schwendenmann L. 2015. Sediment properties and CO<sub>2</sub> efflux from intact and  
579 cleared temperate mangrove forests. *Biogeosciences* 12:6169–80.
- 580 Burdige DJ. 2007. Preservation of organic matter in marine sediments: Controls, mechanisms, and an  
581 imbalance in sediment organic carbon budgets? *Chem Rev* 107:467–85.
- 582 Cahoon DR, Hensel P, Rybczyk J, McKee KL, Proffitt CE, Perez BC. 2003. Mass tree mortality leads to  
583 mangrove peat collapse at Bay Islands, Honduras after Hurricane Mitch. *J Ecol* 91:1093–105.
- 584 Cambi M, Certini G, Neri F, Marchi E. 2015. The impact of heavy traffic on forest soils: A review. *For Ecol*  
585 *Manage* 338:124–38.
- 586 Chave J, Andalo C, Brown S, Cairns MA, Chambers JQ, Eamus D, Fölster H, Fromard F, Higuchi N, Kira T,  
587 Lescure J-P, Nelson BW, Ogawa H, Puig H, Riéra B, Yamakura T. 2005. Tree allometry and improved  
588 estimation of carbon stocks and balance in tropical forests. *Oecologia* 145:87–99.
- 589 Chave J, Coomes D, Jansen S, Lewis SL, Swenson NG, Zanne AE. 2009. Towards a worldwide wood  
590 economics spectrum. *Ecol Lett* 12:351–66.



- 591 Chmura GL, Anisfeld SC, Cahoon DR, Lynch JC. 2003. Global carbon sequestration in tidal, saline wetland  
592 soils. *Global Biogeochem Cycles* 17:1111.
- 593 Clough BF, Scott K. 1989. Allometric relationships for estimating above-ground biomass in six mangrove  
594 species. *For Ecol Manage* 27:117–27.
- 595 Cole TG, Ewel KC, Devoe NN. 1999. Structure of mangrove trees and forests in Micronesia. *For Ecol*  
596 *Manage* 117:95–109.
- 597 Delgado M, de Jonge VN, Peletier H. 1991. Experiments on resuspension of natural microphytobenthos  
598 populations. *Mar Biol* 108:321–8.
- 599 Diochon A, Kellman L, Beltrami H. 2009. Looking deeper: An investigation of soil carbon losses following  
600 harvesting from a managed northeastern red spruce (*Picea rubens* Sarg.) forest chronosequence. *For Ecol*  
601 *Manage* 257:413–20.
- 602 Donato DC, Kauffman JB, Murdiyarso D, Kurnianto S, Stidham M. 2011. Mangroves among the most  
603 carbon-rich forests in the tropics. *Nat Geosci* 4:1–5.
- 604 Drake TW, Van Oost K, Barthel M, Bauters M, Hoyt AM, Podgorski DC, Six J, Boeckx P, Trumbore SE,  
605 Cizungu Ntaboba L, Spencer RGM. 2019. Mobilization of aged and biolabile soil carbon by tropical  
606 deforestation. *Nat Geosci* 12:541–6.
- 607 Duke N, Wolanski E. 2001. Muddy Coastal Waters and Depleted Mangrove Coastlines — Depleted Seagrass  
608 and Coral Reefs. In: Wolanski E, editor. *Oceanographic Processes of Coral Reefs. Physical and Biology*  
609 *Links in the Great Barrier Reef*. Washington, DC: CRC Press. pp 77–91.
- 610 Ellison AM, Farnsworth EJ. 1996. Anthropogenic Disturbance of Caribbean Mangrove Ecosystems: Past  
611 Impacts, Present Trends, and Future Predictions. *Biotropica* 28:549.
- 612 FAO [Food and Agriculture Organization of the United Nations]. 2007. *The world’s mangroves 1980-2005*.  
613 Rome, Italy
- 614 Ferreira TO, Otero XL, de Souza Junior VS, Vidal-Torrado P, Macías F, Firme LP. 2010. Spatial patterns of

- 615 soil attributes and components in a mangrove system in Southeast Brazil (São Paulo). *J Soils Sediments*  
616 10:995–1006.
- 617 Fourqurean JW, Schrlau JE. 2003. Changes in nutrient content and stable isotope ratios of C and N during  
618 decomposition of seagrasses and mangrove leaves along a nutrient availability gradient in Florida Bay,  
619 USA. *Chem Ecol* 19:373–90.
- 620 Gifford RM, Roderick ML. 2003. Soil carbon stocks and bulk density: Spatial or cumulative mass coordinates  
621 as a basis of expression? *Glob Chang Biol* 9:1507–14.
- 622 Gillis LG, Belshe EF, Narayan GR. 2017. Deforested Mangroves Affect the Potential for Carbon Linkages  
623 between Connected Ecosystems. *Estuaries and Coasts* 40:1207–13.
- 624 Glew JR, Smol JP, Last WM. 2001. Sediment Core Collection and Extrusion. In: Last WM, Smol JP, editors.  
625 Tracking Environmental Change Using Lake Sediments: Basin Analysis, Coring, and Chronological  
626 Techniques. Dordrecht: Springer Netherlands, Dordrecht. pp 73–105.
- 627 Granek E, Ruttenberg BI. 2008. Changes in biotic and abiotic processes following mangrove clearing. *Estuar*  
628 *Coast Shelf Sci* 80:555–62.
- 629 Grellier S, Janeau JL, Dang Hoai N, Nguyen Thi Kim C, Le Thi Phuong Q, Pham Thi Thu T, Tran-Thi NT,  
630 Marchand C. 2017. Changes in soil characteristics and C dynamics after mangrove clearing (Vietnam).  
631 *Sci Total Environ* 593–594:654–63.
- 632 Haines WB. 1923. The volume-changes associated with variations of water content in soil. *J Agric Sci*  
633 13:296–310.
- 634 Hamilton SE, Casey D. 2016. Creation of a high spatio-temporal resolution global database of continuous  
635 mangrove forest cover for the 21st century (CGMFC-21). *Glob Ecol Biogeogr* 25:729–38.
- 636 Hargis TG, Twilley RR. 1994. Improved coring device for measuring soil bulk density in a Louisiana deltaic  
637 marsh. *J Sediment Res* 64:681–3.
- 638 Herr D, von Unger M, Laffoley D, McGivern A. 2017. Pathways for implementation of blue carbon

- 639 initiatives. *Aquat Conserv Mar Freshw Ecosyst* 27:116–29.
- 640 IPCC. 2014. 2013 Supplement to the 2006 IPCC Guidelines for National Greenhouse Gas Inventories:  
641 Wetlands Task Force on National Greenhouse Gas Inventories: Wetlands. (Hiraishi T, Krug T, Kiyoto T,  
642 Srivastava N, Jamsranjav B, Fukuda M, Troxler T, editors.). Switzerland: IPCC
- 643 Jamshidi R, Jaeger D, Raafatnia N, Tabari M. 2008. Influence of Two Ground-Based Skidding Systems on  
644 Soil Compaction Under Different Slope and Gradient Conditions. *Int J For Eng* 19:9–16.
- 645 Jones TG, Glass L, Gandhi S, Ravaoarinosihoarana L, Carro A, Benson L, Ratsimba HR, Giri C,  
646 Randriamanatena D, Cripps G. 2016a. Madagascar’s mangroves: Quantifying nation-wide and  
647 ecosystem specific dynamics, and detailed contemporary mapping of distinct ecosystems. *Remote Sens*  
648 8.
- 649 Jones TG, Ratsimba HR, Carro A, Ravaoarinosihoarana L, Glass L, Teoh M, Benson L, Cripps G, Giri C,  
650 Zafindrasilivonona B, Raheindray R, Andriamahenina Z, Andriamahefazafy M. 2016b. The Mangroves  
651 of Ambanja and Ambaro Bays, Northwest Madagascar: Historical Dynamics, Current Status and  
652 Deforestation Mitigation Strategy Trevor. In: Diop S et al., editor. *Estuaries: A Lifeline of Ecosystem*  
653 *Services in the Western Indian Ocean*. Springer International Publishing Switzerland. pp 67–85.
- 654 Jones TG, Ratsimba HR, Ravaoarinosihoarana L, Cripps G, Bey A. 2014. Ecological Variability and  
655 Carbon Stock Estimates of Mangrove Ecosystems in Northwestern Madagascar. *Forests* 5:177–205.
- 656 Kauffman JB, Bernardino AF, Ferreira TO, Bolton NW, Eduardo L, Gabriel DOG, Nobrega N. 2018. Shrimp  
657 ponds lead to massive loss of soil carbon and greenhouse gas emissions in northeastern Brazilian  
658 mangroves. *Ecol Evol* 8:5530–40.
- 659 Kauffman JB, Donato DC. 2012. Protocols for the measurement, monitoring and reporting of structure,  
660 biomass and carbon stocks in mangrove forests. Bogor, Indonesia: CIFOR
- 661 Kauffman JB, Heider C, Norfolk J, Payton F. 2014. Carbon stocks of intact mangroves and carbon emissions  
662 arising from their conversion in the Dominican Republic. *Ecol Appl* 24:518–27.
- 663 Kauffman JB, Hernandez Trejo H, del Carmen Jesus Garcia M, Heider C, Contreras WM. 2016. Carbon

- 664 stocks of mangroves and losses arising from their conversion to cattle pastures in the Pantanos de Centla,  
665 Mexico. *Wetl Ecol Manag* 24:203–16.
- 666 Kauffman JB, Thorpe AS, Brookshire ENJ. 2004. Livestock exclusion and belowground ecosystem responses  
667 in riparian meadows of Eastern Oregon. *Ecol Appl* 14:1671–9.
- 668 Keeling CD. 1979. The Suess effect:  $^{13}\text{C}$ - $^{14}\text{C}$  interrelations. *Environ Int* 2:229–300.
- 669 Kennedy P, Kennedy H, Papadimitriou S. 2005. The effect of acidification on the determination of organic  
670 carbon, total nitrogen and their stable isotopic composition in algae and marine sediment. *Rapid*  
671 *Commun Mass Spectrom* 19:1063–8.
- 672 Komiyama A, Pongpan S, Kato S. 2005. Common allometric equations for estimating the tree weight of  
673 mangroves. *J Trop Ecol* 21:471–7.
- 674 Krauss KW, Cahoon DR, Allen JA, Ewel KC, Lynch JC, Cormier N. 2010. Surface Elevation Change and  
675 Susceptibility of Different Mangrove Zones to Sea-Level Rise on Pacific High Islands of Micronesia.  
676 *Ecosystems* 13:129–43.
- 677 Krishnaswamy S, Lal D, Martin JM, Meybeck M. 1971. Geochronology of lake sediments. *Earth Planet Sci*  
678 *Lett* 11:407–14.
- 679 Kristensen E, Alongi DM. 2006. Control by fiddler crabs (*Uca vocans*) and plant roots (*Avicennia marina*)  
680 on carbon, iron, and sulfur biogeochemistry in mangrove sediment. *Limnol Oceanogr* 51:1557–71.
- 681 Labrière N, Locatelli B, Laumonier Y, Freycon V, Bernoux M. 2015. Soil erosion in the humid tropics: A  
682 systematic quantitative review. *Agric Ecosyst Environ* 203:127–39.
- 683 Lang'at JKS, Kairo JG, Mencuccini M, Bouillon S, Skov MW, Waldron S, Huxham M. 2014. Rapid losses of  
684 surface elevation following tree girdling and cutting in tropical mangroves. *PLoS One* 9:1–8.
- 685 Lovelock CE, Atwood T, Baldock J, Duarte CM, Hickey S, Lavery PS. 2017a. Assessing the risk of carbon  
686 dioxide emissions from blue carbon ecosystems. *Front Ecol Environ* 15:257–65.
- 687 Lovelock CE, Fourqurean JW, Morris JT. 2017b. Modeled CO<sub>2</sub> Emissions from Coastal Wetland Transitions

- 688 to Other Land Uses: Tidal Marshes, Mangrove Forests, and Seagrass Beds. *Front Mar Sci* 4:1–11.
- 689 Lovelock CE, Ruess R, Feller I. 2011. CO<sub>2</sub> efflux from cleared mangrove peat. *PLoS One* 6:e21279.
- 690 Lundquist CJ, Morrissey DJ, Gladstone-Gallagher R V., Swales A. 2014. Managing Mangrove Habitat  
691 Expansion in New Zealand. In: *Mangrove Ecosystems of Asia*. New York, NY: Springer New York. pp  
692 415–38.
- 693 Macnae W. 1969. A General Account of the Fauna and Flora of Mangrove Swamps and Forests in the Indo-  
694 West-Pacific Region. *Adv Mar Biol* 6:73–270.
- 695 Maher DT, Call M, Santos IR, Sanders CJ. 2018. Beyond burial: Lateral exchange is a significant atmospheric  
696 carbon sink in mangrove forests. *Biol Lett* 14.
- 697 Maher DT, Santos IR, Schulz KG, Call M, Jacobsen GE, Sanders CJ. 2017. Blue carbon oxidation revealed by  
698 radiogenic and stable isotopes in a mangrove system. *Geophys Res Lett* 44:4889–96.
- 699 McKee KL. 2011. Biophysical controls on accretion and elevation change in Caribbean mangrove  
700 ecosystems. *Estuar Coast Shelf Sci* 91:475–83.
- 701 McLeod E, Chmura GL, Bouillon S, Salm R, Björk M, Duarte CM, Lovelock CE, Schlesinger WH, Silliman  
702 BR. 2011. A blueprint for blue carbon: Toward an improved understanding of the role of vegetated  
703 coastal habitats in sequestering CO<sub>2</sub>. *Front Ecol Environ* 9:552–60.
- 704 Middelburg JJ. 2018. Reviews and syntheses: To the bottom of carbon processing at the seafloor.  
705 *Biogeosciences* 15:413–27.
- 706 Morton RA, White WA. 1997. Characteristics of and corrections for core shortening in unconsolidated  
707 sediments. *J Coast Res* 13:761–9.
- 708 Ong JE. 1993. Mangroves - a carbon source and sink. *Chemosphere* 27:1097–107.
- 709 Osland MJ, Spivak AC, Nestlerode JA, Lessmann JM, Almario AE, Heitmuller PT, Russell MJ, Krauss KW,  
710 Alvarez F, Dantin DD, Harvey JE, From AS, Cormier N, Stagg CL. 2012. Ecosystem Development  
711 After Mangrove Wetland Creation: Plant-Soil Change Across a 20-Year Chronosequence. *Ecosystems*

- 712 15:848–66.
- 713 Otero XL, Méndez A, Nóbrega GN, Ferreira TO, Meléndez W, Macías F. 2017. High heterogeneity in soil  
714 composition and quality in different mangrove forests of Venezuela. *Environ Monit Assess* 189.
- 715 Rasolofo M, Ramilijaona O. 2009. Variability in the abundance and recruitment of *Fenneropenaeus indicus*  
716 and *Metapenaeus monoceros* postlarvae and juveniles in Ambaro Bay mangroves of Madagascar. *Nat*  
717 *Faune* 24:103–9.
- 718 Sanchez-Cabeza JA, Masqué P, Ani-Ragolta I. 1998. <sup>210</sup>Pb and <sup>210</sup>Po analysis in sediments and soils by  
719 microwave acid digestion. *J Radioanal Nucl Chem* 227:19–22.
- 720 Semeniuk V. 1996. Coastal forms and Quaternary processes along the arid Pilbara coast of northwestern  
721 Australia. *Palaeogeogr Palaeoclimatol Palaeoecol* 123:49–84.
- 722 Sidik F, Lovelock CE. 2013. CO<sub>2</sub> Efflux from Shrimp Ponds in Indonesia. *PLoS One* 8:6–9.
- 723 Sippo JZ, Maher DT, Schulz KG, Sanders CJ, McMahon A, Tucker J, Santos IR. 2019. Carbon outwelling  
724 across the shelf following a massive mangrove dieback in Australia: Insights from radium isotopes.  
725 *Geochim Cosmochim Acta* 253:142–58.
- 726 Stover HJ, Henry HAL. 2018. Soil homogenization and microedges: perspectives on soil-based drivers of  
727 plant diversity and ecosystem processes. *Ecosphere* 9:e02289.
- 728 Taillardat P, Friess DA, Lupascu M. 2018. Mangrove blue carbon strategies for climate change mitigation are  
729 most effective at the national scale. *Biol Lett* 14:20180251.
- 730 Thampanya U, Vermaat JE, Sinsakul S, Panapitukkul N. 2006. Coastal erosion and mangrove progradation of  
731 Southern Thailand. *Estuar Coast Shelf Sci* 68:75–85.
- 732 Twilley RR, Day JW. 2012. Mangrove Wetlands. In: W. Day J, C. Crump B, Kemp WM, Yáñez-Arancibia A,  
733 editors. *Estuarine Ecology*. Second. Hoboken, NJ, USA: John Wiley & Sons, Inc. pp 165–202.
- 734 Wendt JW, Hauser S. 2013. An equivalent soil mass procedure for monitoring soil organic carbon in multiple  
735 soil layers. *Eur J Soil Sci* 64:58–65.

- 736 Wentworth C. 1922. A scale of grade and class terms for clastic sediments. *J Geol* 30:377–92.
- 737 Yanai RD, Currie WS, Goodale CL. 2003. Soil carbon dynamics after forest harvest: An ecosystem paradigm  
738 reconsidered. *Ecosystems* 6:197–212.
- 739 Zanne AE, Lopez-Gonzalez G, Coomes DA, Ilic J, Jansen S, Lewis SL, Miller RB, Swenson NG, Wiemann  
740 MC, Chave J. 2009. Data from: towards a worldwide wood economics spectrum. Dryad Digit Repos.
- 741 Zummo LM, Friedland AJ. 2011. Soil carbon release along a gradient of physical disturbance in a harvested  
742 northern hardwood forest. *Ecol Manage* 261:1016–26.
- 743

744 **Table Legends**

745 **Table 1. Site characteristics for sampled mangrove plots of Tsimipaika Bay, Madagascar.**

746 Average values for tree height (m), diameter at breast height (dbh) (cm) and trees per hectare ( $\text{ha}^{-1}$ ).

747 Dead tree density in deforested plots equals stump density and regeneration density equals number of  
748 seedlings per unit area. Cc stands for Closed-canopy, De for Deforested, and n.d. for “no data”.

749

750 **Table 2. Intact and deforested soil characteristics over the upper  $45 \text{ g}\cdot\text{cm}^{-2}$ .** U and t values of

751 Mann-Witney and Two-sample t- test results are included for the comparison of soil properties

752 between intact and deforested mangrove soils. \*\*\*Significant at 0.001 level, \*\* at 0.01 and \* at 0.05.

753 NS is not significant.

754

755 **Table 3. Sedimentation rates and  $^{210}\text{Pb}_{\text{xs}}$  inventories in intact and deforested soils.** The

756 uncertainties represent the SE resulting from the CF:CS model to obtain the mass accumulation and

757 accretion rates (MAR and SAR), and  $^{226}\text{Ra}$  specific activities represent the mean and the standard

758 deviation ( $n = 5$  at each core). Accretion rates (SAR) were corrected for core shortening thus should

759 be considered as apparent rates.

760

761 **Table 4. Soil carbon and nitrogen accumulation rates and stocks.** Stocks in the upper 1 meter are

762 also included for reporting purposes and should be considered apparent stocks due to the soil

763 shortening correction applied.

764

765 **Table 5. Published C loss rates from degraded mangrove soils.** To facilitate comparison among

766 most other assessments and this study, C losses are expressed as  $\text{CO}_2$  equivalents ( $\text{CO}_2\text{e}$ ) obtained by

767 multiplying C loss rate by 3.67. Where rates of C loss were not reported, we estimated a mean annual

768 C loss as the total soil C stock loss divided by the time since disturbance.



769 **Table 1.**

Core ID	Species dominance	Geomorphic position	Tidal inundation	Tree height (m)	dbh (cm)	Live Tree Density (ha <sup>-1</sup> )	Dead Tree Density (ha <sup>-1</sup> )	Regeneration density (ha <sup>-1</sup> )	Canopy cover (%)	Total biomass C (Mg C ha <sup>-1</sup> )
Cc18	<i>S. alba</i>	Riverine	freq.	8	18	800	0	0	94	160
Cc19	<i>B. gymnorhiza</i>	Riverine	infreq.	10	13	2400	200	5200	95	254
Cc20	<i>R. mucronata</i>	Basin	freq.	9	10	4700	200	800	95	238
Cc28	<i>R. mucronata</i>	Basin	infreq.	n.d.	10	2900	400	2800	93	128
Cc29	<i>R. mucronata</i>	Riverine	freq.	9	9	2900	600	0	98	113
De27	<i>B. gymnorhiza</i>	Riverine	freq.	5	7	200	100	0	0.9	3.0
De30	<i>B. gymnorhiza</i>	Basin	infreq.			0	1000	2000	0.2	1.8
De31	<i>R. mucronata</i>	Basin	freq.			0	100	0	0.2	0.1
De32	<i>C. tagal</i>	Riverine	infreq.			0	3000	2400	7	1.4
De33	<i>C. tagal</i>	Basin	infreq.			0	11400	4400	0.2	9.5

770

771 **Table 2.**

Soil Class	Core ID	Statistic	Water content (%)	DBD (g cm <sup>-3</sup> )	C (%DW)	N (%DW)	C:N	Clay (%)
High-DBD Intact	Cc19, 20	Mean ± SE	30.1 ± 0.6	0.881 ± 0.013	2.40 ± 0.08	0.095 ± 0.003	28.6 ± 0.6	11.2 ± 1.0
		Median	29.1	0.88	2.3	0.093	28.0	10.3
Low-DBD Intact	Cc18, 28, 29	Mean ± SE	56.9 ± 0.7	0.347 ± 0.008	7.7 ± 0.2	0.314 ± 0.012	29.6 ± 0.4	15.3 ± 1.1
		Median	58.7	0.36	7.4	0.30	28.9	15
Intact (all)	Cc18, 19, 20, 28, 29	Mean ± SE	47.4 ± 0.9	0.580 ± 0.015	5.7 ± 0.2	0.231 ± 0.011	29.3 ± 0.3	14.0 ± 0.8
		Median	48.7	0.49	5.5	0.20	28.8	13.1
Deforested	De27, 30, 31, 32, 33	Mean ± SE	44.5 ± 0.4	0.415 ± 0.006	5.11 ± 0.15	0.173 ± 0.003	33.5 ± 0.6	28.1 ± 1.3
		Median	44.3	0.41	4.8	0.17	32.6	26.4
Treatment					Prob> U			Prob> t
Intact (all) vs. Deforested			0.007 **	1.1·10 <sup>-9</sup> ***	1.00 NS	0.11 NS	2.6·10 <sup>-8</sup> ***	1.1·10 <sup>-14</sup> ***
High-DBD Intact vs. Deforested			0 ***	5.6·10 <sup>-53</sup> ***	4.1·10 <sup>-26</sup> ***	1.7·10 <sup>-25</sup> ***	7.0·10 <sup>-6</sup> ***	9.4·10 <sup>-10</sup> ***
Low-DBD Intact vs. Deforested			0 ***	2.6·10 <sup>-9</sup> ***	0***	0***	2.6·10 <sup>-6</sup> ***	3.4·10 <sup>-10</sup> ***

772

773

774

775 **Table 3.**

Core ID	Type	Mixing depth	<sup>210</sup> Pb <sub>xs</sub> horizon	<sup>226</sup> Ra	MAR	SAR	<sup>210</sup> Pb <sub>xs</sub> inventory
		g cm <sup>-2</sup>	g cm <sup>-2</sup>	Bq kg <sup>-1</sup>	g cm <sup>-2</sup> yr <sup>-1</sup>	mm yr <sup>-1</sup>	Bq m <sup>-2</sup>
Cc19	High-DBD	1.7	7	13.2 ± 1.5	0.070 ± 0.014	0.85 ± 0.11	500 ± 50
Cc20		2.0	9	12.6 ± 1.3	0.099 ± 0.013	1.11 ± 0.15	690 ± 40
Cc18	Low-DBD	0.8	11	19 ± 4	0.094 ± 0.007	4.1 ± 0.2	3170 ± 90
Cc28		1.2	13	13 ± 4	0.10 ± 0.02	2.3 ± 0.4	1920 ± 80
Cc29		1.5	17	13 ± 2	0.223 ± 0.012	8.4 ± 0.4	4750 ± 80
<b>Mean (SE) high-DBD</b>		<b>1.9 ± 0.2</b>	<b>8.0 ± 0.8</b>		<b>0.085 ± 0.015</b>	<b>0.98 ± 0.13</b>	<b>600 ± 100</b>
<b>Mean (SE) low-DBD</b>		<b>1.2 ± 0.2</b>	<b>13 ± 2</b>		<b>0.14 ± 0.04</b>	<b>5 ± 2</b>	<b>3280 ± 820</b>
<b>Mean (SE) Intact</b>		<b>1.4 ± 0.2</b>	<b>11 ± 2</b>		<b>0.12 ± 0.03</b>	<b>3.4 ± 1.4</b>	<b>2210 ± 800</b>
De27	Deforested	4	14	25 ± 6			1940 ± 90
De30		6	14	18 ± 4			1200 ± 70
De31		25	24	13.0 ± 1.4			2580 ± 90
De32		8	10	21 ± 6			1870 ± 170
De33		26	26	15 ± 2			2040 ± 100
<b>Mean (SE) Deforested</b>		<b>14 ± 5</b>	<b>18 ± 3</b>				<b>1930 ± 220</b>

776

777 **Table 4.**

Core ID	Type	C accumulation rate		N accumulation rate		C stock		N stock		C stock	N stock
		g C m <sup>-2</sup> yr <sup>-1</sup>		g N m <sup>-2</sup> yr <sup>-1</sup>		0-14 g cm <sup>-2</sup>	0-45 g cm <sup>-2</sup>	0-14 g cm <sup>-2</sup>	0-45 g cm <sup>-2</sup>	1 m	1 m
						Mg C ha <sup>-1</sup>		Mg N ha <sup>-1</sup>		Mg C ha <sup>-1</sup>	Mg N ha <sup>-1</sup>
Cc19	High-DBD	18	± 4	0.68	± 0.14	32	109	1.3	4.1	218	8
Cc20		25	± 3	1.18	± 0.15	33	91	1.5	3.9	192	8
Cc18	Low-DBD	75	± 6	3.4	± 0.3	108	279	4.4	11	190	7
Cc28		64	± 11	2.2	± 0.4	87	248	3.1	8.9	250	9
Cc29		176	± 9	7.3	± 0.4	135	305	5.8	13	229	9
<b>Mean (SE) High-DBD Intact</b>		<b>21</b>	<b>± 3</b>	<b>0.9</b>	<b>± 0.3</b>	<b>32.4 ± 0.4</b>	<b>100 ± 9</b>	<b>1.40 ± 0.12</b>	<b>3.99 ± 0.06</b>		
<b>Mean (SE) Low-DBD Intact</b>		<b>110</b>	<b>± 40</b>	<b>4</b>	<b>± 2</b>	<b>110 ± 14</b>	<b>280 ± 20</b>	<b>4.4 ± 0.8</b>	<b>11.0 ± 1.1</b>		
<b>Mean (SE) Intact</b>		<b>70</b>	<b>± 30</b>	<b>3.0</b>	<b>± 1.2</b>	<b>80 ± 20</b>	<b>200 ± 40</b>	<b>2.9 ± 0.8</b>	<b>8 ± 2</b>	<b>220 ± 10</b>	<b>8.3 ± 0.3</b>
De27	Deforested					64	268	2.1	8	268	8
De30						69	344	2.2	10	279	8
De31						53	194	2.1	7	181	6
De32						57	261	3.1	10	166	6
De33						52	170	2.2	7	135	5
<b>Mean (SE) deforested</b>						<b>60 ± 3</b>	<b>250 ± 30</b>	<b>2.3 ± 0.2</b>	<b>8.2 ± 0.7</b>	<b>210 ± 30</b>	<b>7.0 ± 0.5</b>

778

779 **Table 5.**

References	Disturbance type	Years since disturbance	Method for estimating C loss	CO <sub>2</sub> emissions		
				Mg CO <sub>2</sub> e ha <sup>-1</sup> yr <sub>i</sub> <sup>-1</sup>		
<b>This study</b>	<b>Clearing</b>	<b>10</b>	<b>C stock change</b>	<b>18</b>	<b>±</b>	<b>5</b>
Grellier and others (2017)	Clearing	2	C stock change	37		
Bulmer and others (2015)	Clearing	0.1-8	Gas flux chambers	4	±	7
Lang'at and others (2014)	Clearing	2	C stock change	21	±	6
			Gas flux chambers	35	±	45
Lovelock and others (2011)	Clearing	1	Gas flux chambers	25	±	7
		20		106		
		30		30		
Kauffman and others (2016b)	Conversion to cattle pastures	7	C stock change	16	±	6
		30		7	±	2
Kauffman and others (2014)	Conversion to aquaculture	29	C stock change	82		
		10-12		107	±	40
Kauffman and others (2018)	Conversion to aquaculture	10-12	C stock change	184	±	10
		8		13	±	5
Sidik and Lovelock (2013)	Conversion to aquaculture	25	Gas flux chambers in pond floor	16		
			Gas flux chambers in pond walls	44		
Cahoon and others (2003)	Hurricane damage	2	Change in soil volume	19		

780

781

782 **Figure Legends**

783 **Figure 1.** Map of Tsimipaika Bay in northwest Madagascar with sampled plot locations in  
784 intact and deforested mangrove areas. St. labels are surface water sampling locations.

785

786 **Figure 2.** Principal component analysis on physico-chemical properties of soils from  
787 deforested and intact mangroves. Biplot of variable vectors showing correlation between the  
788 variables, the component and individual factor map. Superimposed on the plot are the  
789 confidence ellipses for categorical variables: deforested soils (orange circles), low-DBD  
790 intact mangrove soils (grey squares) and high-DBD intact mangrove soils (black triangles).

791

792 **Figure 3.** Concentrations of DOC in surface water at 8 stations along the shores of the intact  
793 and deforested mangrove areas.

794

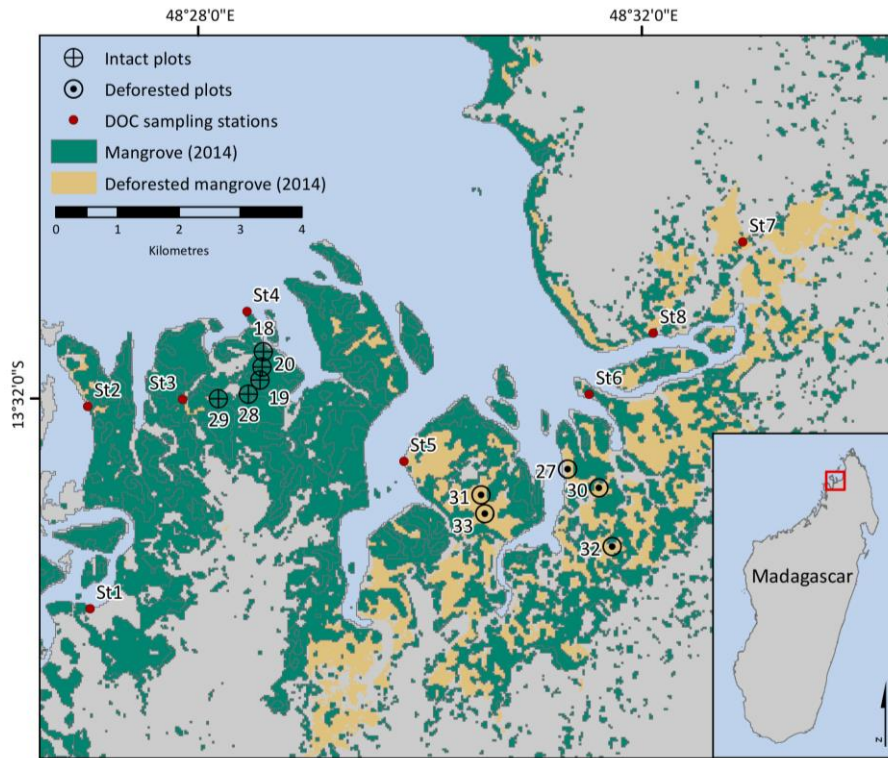
795 **Figure 4.** Soil properties (bulk density, water, carbon and nitrogen contents) with cumulative  
796 mass in intact and deforested mangrove soils. Insets contain soil carbon ( $\delta^{13}\text{C}$ ) and nitrogen  
797 ( $\delta^{15}\text{N}$ ) stable isotopes with cumulative mass in a low-DBD intact and a deforested mangrove  
798 soil. The line at  $14 \text{ g cm}^{-2}$  indicates the separation between the upper and bottom reference  
799 soil mass layers.

800

801 **Figure 5.** Excess  $^{210}\text{Pb}$  specific activity profiles with cumulative mass in intact (a) and  
802 deforested mangrove soils (b). The filled area illustrates excess  $^{210}\text{Pb}$  inventories.

803

804 **Figure 6.** Total ecosystem C stocks of intact and deforested mangrove forests of Tsimipaika  
805 Bay, Madagascar. C stocks to 1 m have been corrected for shortening during coring as  
806 described in the Methods and should be considered apparent C stocks.

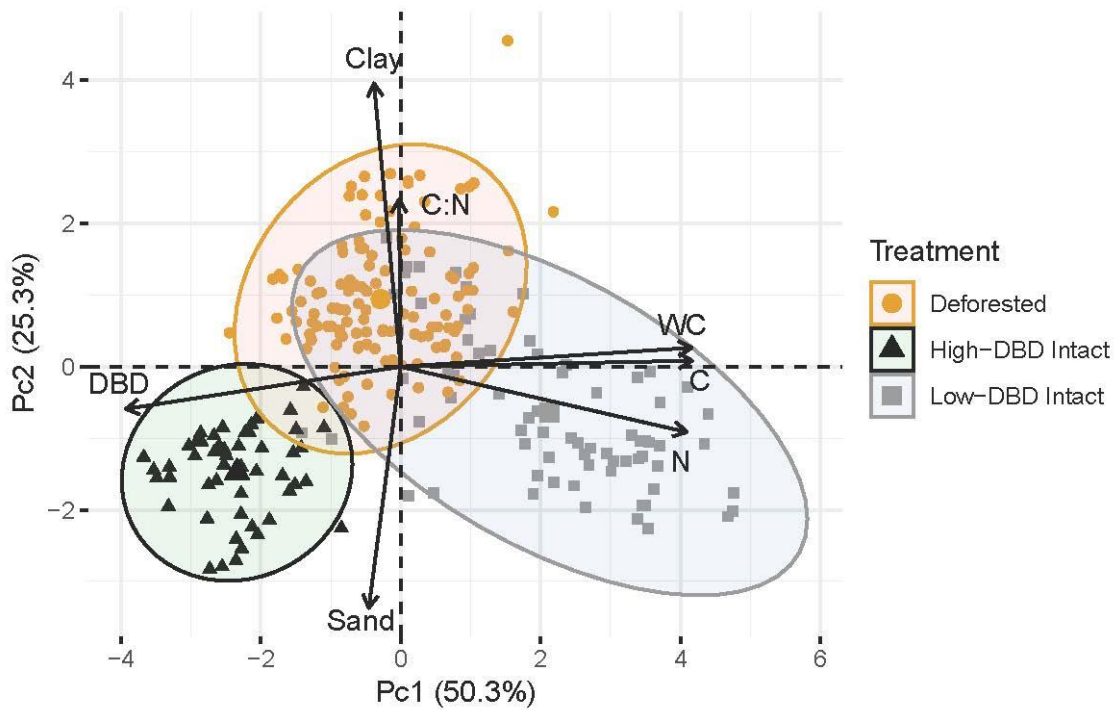


807

808

809

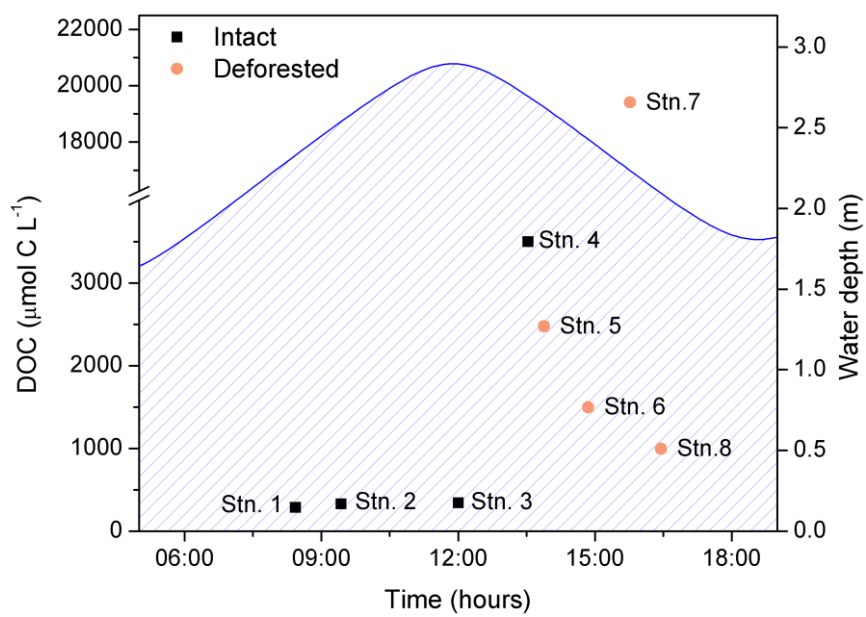
Figure 1



810

811

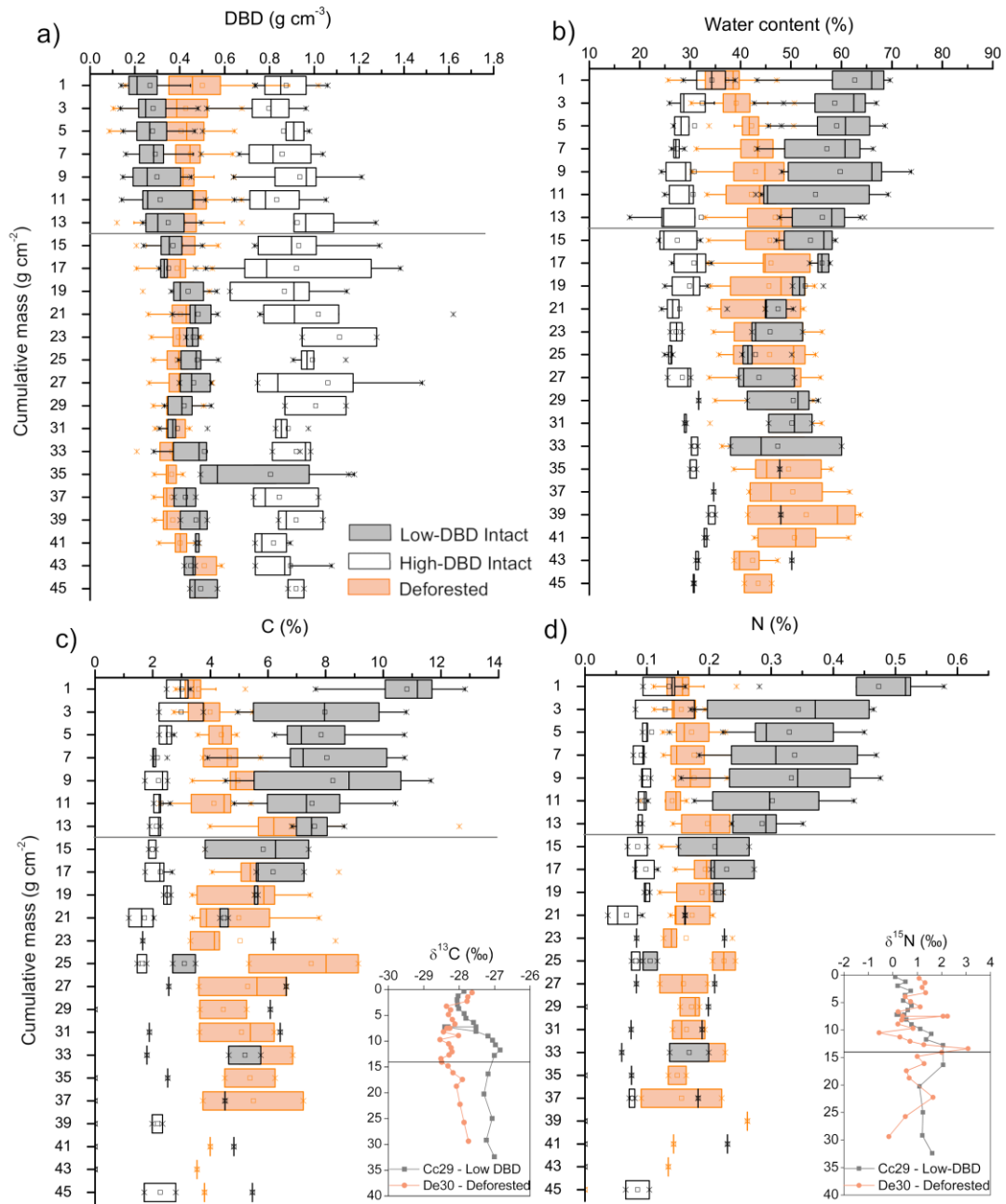
Figure 2



812

813

Figure 3

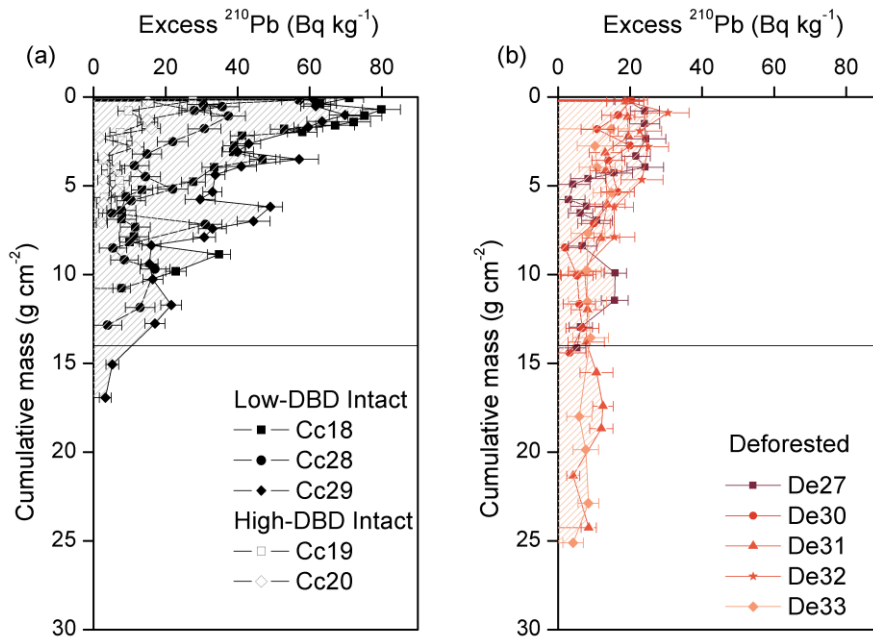


814

815

Figure 4



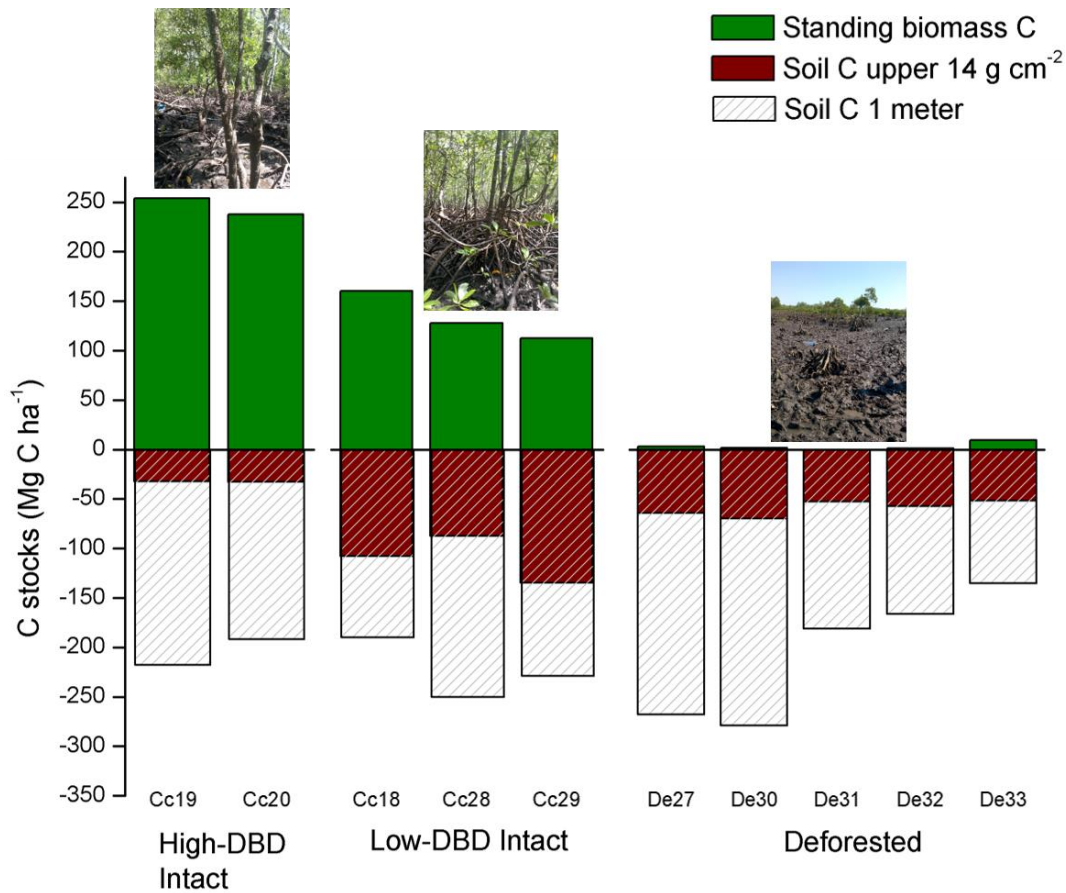


816

817

818

Figure 5



819

820

Figure 6